

Multiple Morphologies of "Crew-Cut" Aggregates of Polystyrene-*b*-poly(acrylic acid) Block Copolymers

Lifeng Zhang and Adi Eisenberg*

The observation by transmission electron microscopy of six different stable aggregate morphologies is reported for the same family of highly asymmetric polystyrene-poly(acrylic acid) block copolymers prepared in a low molecular weight solvent system. Four of the morphologies consist of spheres, rods, lamellae, and vesicles in aqueous solution, whereas the fifth consists of simple reverse micelle-like aggregates. The sixth consists of up to micrometer-size spheres in aqueous solution that have hydrophilic surfaces and are filled with the reverse micelle-like aggregates. In addition, a needle-like solid, which is highly birefringent, is obtained on drying of aqueous solutions of the spherical micelles. This range of morphologies is believed to be unprecedented for a block copolymer system.

Small molecule amphiphile surfactant systems can form aggregates or micelles of various morphologies (1). Also, depending on the block copolymer composition, multiple morphologies exist in the bulk phase of block copolymers (2, 3), in block copolymer-homopolymer blends (4), and in two-dimensional micelle systems of amphiphilic block copolymers on water surfaces (5). In block copolymer solutions, spherical micelles have been identified in many studies (6, 7). However, nonspherical micelles in solution have been observed only rarely and mostly indirectly (8, 9). To our knowledge, multiple morphologies, that is, spheres, rods, and vesicles or lamellae, have not yet been seen for the same block copolymer family in solutions of low molecular weight solvents. In this report, we describe the preparation and observation of six different morphologies. All of these were prepared in a low molecular weight solvent system from block copolymers of the same type differing only in the relative block lengths. This factor may allow for more precise modeling studies of the dependence of the morphologies on the molecular architecture in such system in solution. Four of the morphologies consist of spheres, rods, lamellae, and vesicles in aqueous solution, while the fifth consists of simple reverse micelle-like aggregates in organic solvents. The sixth is new and consists of large spheres in aqueous solution that have hydrophilic surfaces and are filled with reverse micelle-like aggregates. In addition to these six different morphologies, a needle-like solid, which is highly birefringent, was obtained by drying aqueous solutions of the spherical micelles of the block copolymers. This range of mor-

phologies is unprecedented for block copolymer systems.

The polymers used in this study are diblocks of polystyrene (PS) and poly(acrylic acid) (PAA), which we synthesized by anionic polymerization as described before (10). The polydispersity indices of the copolymers, estimated by gel permeation chromatography, were between 1.04 to 1.05. To prepare the colloidal aqueous solutions, deionized water at a rate of one drop every 10 s was added with vigorous stirring to a solution of the copolymer (2 weight %, 10 ml) in *N,N*-dimethylformamide (DMF). Addition of water was continued until 25 weight % of water had been

added. The quality of the solvent for the PS block worsened as the addition of water progressed. Micellization occurred when the water content reached ~5 weight %. The resulting solution was placed in a dialysis bag [Spectra/Por; molecular weight (M_w) cutoff of 8000] and dialyzed against distilled water for 4 days to remove DMF. Transmission electron microscopy (TEM) was performed with a Phillips EM410 microscope operating at an acceleration voltage of 80 kV (11).

Several of the morphologies described here (with the exception of the vesicles) resemble micelles; however, they should be referred to as micelle-like aggregates (MLAs) because, after preparation under equilibrium conditions and subsequent isolation in water, they are no longer in thermodynamic equilibrium; once the organic solvent is removed, the PS cores are below their glass transition temperature T_g . However, much of the block copolymer literature refers to the nonequilibrium block copolymer MLAs as micelles, in recognition of the structural similarities to equilibrium micellar associates. This convention is adopted in this report. The name "crew-cut" (12, 13) was suggested for the system under study because the length of the corona-forming block (PAA) of the aggregates is very short compared to that of the core-forming block (PS). The compositions of the blocks are indicated by *x-b-y*, where *x* is the number of styrene units and *y* is the number of acrylic acid units in the chain.

Figure 1 shows the four morphologies of

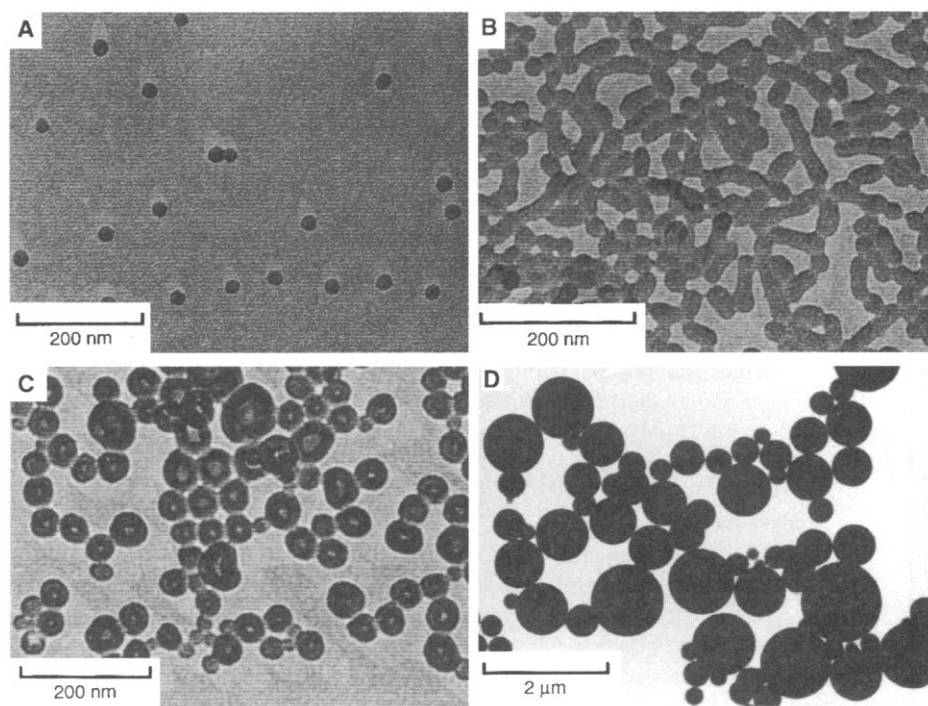


Fig. 1. Multiple morphologies of the crew-cut aggregates from block copolymers of (A) 200-*b*-21, (B) 200-*b*-15, (C) 200-*b*-8, and (D) 200-*b*-4.

Department of Chemistry, McGill University, 801 Sherbrooke Street West, Montreal, Quebec, H3A-2K6, Canada.

*To whom correspondence should be addressed.

the aggregates prepared from block copolymers of different compositions that contain the same polystyrene block. The least asymmetric diblock copolymer (200-*b*-21) gives spherical micelles of low polydispersity (Fig. 1A). They consist of a PS core (26-nm average diameter) with the surface covered by the PAA chains forming the corona. This is the most common morphology reported for block copolymer micelles in which, in contrast with the present system, the corona is normally larger than the core. Very recently, the preparation of spherical "crew-cut" micelles of the type encountered here but made from polystyrene-*b*-poly(4-vinylpyridinium methyl iodide) was reported (13). As the PAA block length decreases to 15 (200-*b*-15), the morphology changes from spherical to rod-like (23 nm in diameter) (Fig. 1B). The morphology changes again from rod-like to vesicular (Fig. 1C) when the PAA block length decreases still further (200-*b*-8). The vesicular nature is evidenced from a higher transmission in the center of the aggregates than around their periphery, coupled with height measurements (from shadowing) which show the aggregates to be spherical. The sizes of the vesicles are quite polydisperse, with diameters up to 100 nm. However, the PS wall thickness of the vesicles is very uniform (18 ± 2 nm). Finally, Fig. 1D shows the micelles from the block copolymer with the shortest PAA block length (200-*b*-4). These micelles are spherical, solid, highly polydisperse and contain some very large

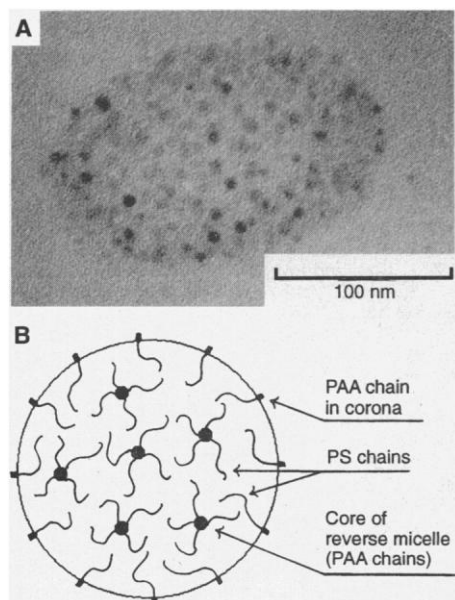


Fig. 2. (A) The internal morphology of the large complex micelle made from the block copolymer (200-*b*-4) in Fig. 1D. The elongation of the particle shape in one direction is probably caused by the strong shear forces during microtoming. (B) A schematic structure of the large complex micelle filled with bulk reverse micelles.

specimens (up to 1200 nm diameter in this image). A micrograph of a section of one of the smaller spheres, along with a schematic picture (Fig. 2), shows that the sphere has an internal structure similar to that of block copolymers cast from a solution in a solvent in which the blocks form reverse micelles, with the polar cores on the inside and the styrene in the corona (2). These inverse micelles are, in principle, the phase-inverted versions of the aqueous crew-cut micelles. Such reverse micelles in salt form are soluble in a range of organic solvents and retain their identity in solution indefinitely at room temperature (14). Because this block ionomer reverse micelle morphology has been explored extensively in bulk and in solution (14, 15), it will not be described further. The large spheres with hydrophilic surfaces, which makes them stable in aqueous solution, however, are new. Note that the schematic shows a superficial resemblance to a mammalian cell, as well as to the structure of high-impact polystyrene (HIPS) (16).

Examination of micrographs of the aggregates in the range of compositions that give vesicles occasionally reveals lamellar micelles. An example is shown in Fig. 3 for the block copolymer 410-*b*-16. The thickness of the lamella (24 nm) is of the same order as the wall thickness of the vesicles (22 nm), as evidenced from the length of the shadowed region.

Although the existence of vesicles made of block copolymers in low molecular weight solvents has been postulated individually on the basis of indirect evidence

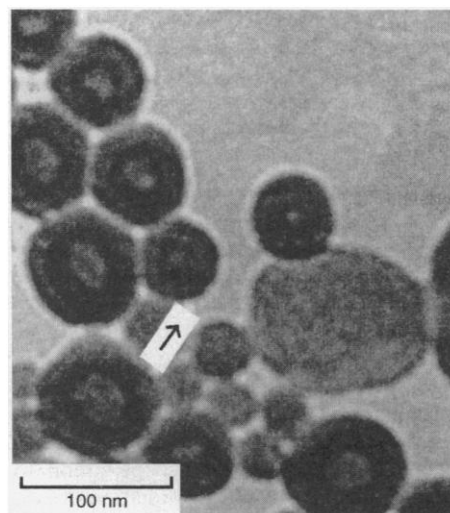


Fig. 3. The morphologies of the aggregates made from the diblock copolymer 410-*b*-16. One lamellar micelle can be seen among the vesicles. The lamellar nature is evidenced by the uniformity of the light intensity over the entire feature. The wall thickness of the vesicles and the thickness of the lamellar micelle are consistent (22 versus 24 nm). The arrow indicates the direction of shadowing.

(9), these structures have been observed directly by electron microscopy. Furthermore, we are not aware of any method of preparing glassy ($T_g \approx 100^\circ\text{C}$) vesicles of this type (that is, size, wall thickness, and composition) by techniques other than that described here. The preparation of all of the morphologies (except the lamellae) is very reproducible. Furthermore, depending on the soluble chain length, the same morphologies can be observed for block copolymer series with different PS chain lengths. The boundaries, in terms of percentage by mole of PAA block content between the different morphological regions, do not appear to change with PS block length for the samples we have studied.

For blends of poly(styrene-*b*-butadiene) diblocks with homopolystyrene (in which the butadiene forms the discontinuous phase), Kinning *et al.* (4) reported that the morphology can change from spherical to cylindrical and eventually to vesicular, by increasing either the insoluble butadiene block content in the block copolymer or the homopolystyrene molecular weight. By extrapolating the reported trends, nonspherical morphologies of block copolymer aggregates can be expected in low molecular weight solvents only if the soluble block of the copolymer is very short, with the long block remaining insoluble. However, for these very short block lengths, differential solubility in nonaqueous block copolymer systems may be very difficult to achieve. Furthermore, even if it is achieved, the isolation of the aggregates into a form in which they can be stabilized and dried may be even more difficult. Therefore, it has not been possible to make stable block copolymer vesicles (which can be isolated and dried), either in water or in other small molecule solvents. In the present system, however, it is possible to do so because of the large difference in the solubilities of the hydrophilic and hydrophobic blocks. Once formed in their various morphologies at equilibrium, the aggregates can be deswelled in water, which makes them very stable because of the strong interactions between the acidic or ionic aqueous corona-forming PAA blocks and the water. Also, at room temperature, the deswelled cores are probably well below the T_g of bulk PS.

Thermodynamically, the present system in aqueous solution is not an equilibrium system. However, the multiple morphologies, as well as the dimensions, are a result of a thermodynamic equilibrium that prevailed while the equilibrium micelles or vesicles were being formed in DMF at low water contents during water addition. The different morphologies are thus a manifestation of the thermodynamics during the aggregation process. During aggregation, the cores (styrene-rich regions) would be

expected to be swollen by a DMF-rich solvent mixture. As the solvent is removed from the swollen PS cores during the addition of water and the subsequent dialysis, the cores pass the glass transition at room temperature, at which point the core structures become locked. In view of the above, it seems reasonable to think that the morphologies and dimensions seen in Fig. 1 are directly related to those of the swollen cores in the equilibrium state, although they are obviously not identical.

In the block copolymer micelles, the major contributions to the thermodynamics of aggregation are considered to originate mainly from three sources, namely, the core, the interaction between the corona and the solvent, and the core-solvent interface (7). Among these, the contribution of the core, which is influenced by a number of factors, may be the most variable, considering the range of core dimensions and morphologies seen here. The PS chains in the spherical core are stretched in the radial direction compared with their dimensions in the unperturbed state. The degree of stretching is probably proportional to the radius of the micelle core. Therefore, from the dimensions of the various structures in Fig. 1, it is of interest to estimate how the degree of the stretching of the core-forming PS chains (in the unswollen state) changes as the morphologies change. The stretching

of the PS chains is greatest in the spherical micelles (the ratio of the core radius to the chain end-to-end distance in the unperturbed state being 1.4); the stretching decreases as the shape changes from spherical to rod-like (ratio = 1.25), and decreases still further as vesicles or lamellae are formed (ratio = 1.0). These ratios are expected to be related to a comparable stretching parameter while the micelles are formed under equilibrium conditions. It has been found experimentally (17), and also suggested on theoretical grounds (18), that the radius of the spherical core increases with a decrease of the corona-forming block length at a constant PS block length, implying a corresponding increase of the degree of stretching of the PS block. Because the stretching results in a decrease in the entropy of the PS chains in the micelle core, it cannot continue indefinitely as the soluble block (PAA) length decreases. At some point, the system becomes unstable (18). This might explain qualitatively the behavior of the present system. Beyond a certain degree of stretching, the morphology changes first from spherical to rod-like, and eventually to lamellar or vesicular, presumably to reduce the thermodynamic stretching penalty.

It is of interest to study theoretically the relations between structural parameters of block copolymer micelles (7, 18, 19), the transition between the different morphologies (20), and the molecular characteristics of the constituent block copolymers. The present system can serve as an experimental reference point for these studies because all of the transitions have been identified. From a practical point of view, it is anticipated that, because of the size and the degree of control that can be exercised over the organic core, the crew-cut micelles may adsorb or release organic chemicals (such as drugs) from or into aqueous solutions with a range of rates. They may thus be useful in the treatment of waste water, or serve as controlled delivery vehicles for hydrophobic drugs. In connection with the latter, the large spheres filled with inverse micelles might be most interesting. They are hydrophilic; however, depending on the composition of the long block, they might be expected to break down into their constituent reverse micelles in a hydrophobic environment, such as in lipids, thus providing a possible targeting mechanism. The intravesicular cavities might also be useful in drug delivery. Finally, the formation of vesicles and especially of the large complex micelles that have a superficial resemblance to cells, not only in appearance but also in size, may be of some interest in the life sciences, since hydrophilic regions form in a hydrophobic matrix which, in turn, is surrounded by a hydrophilic surface.

In addition to the six morphologies de-

scribed above, we have also prepared a needle-like solid, which forms at the glass-air interface when a solution of the spherical micelles is dried. An optical micrograph (Fig. 4A) of the appearance of the crack pattern in the dried layer shows that the arrangement of these features is very regular. Soaking the cracked film in water results in a desorption of the needles, which are now highly birefringent (Fig. 4B). The first-order birefringence colors (yellow and blue) can be observed by using a first-order red plate, which indicates that the needles have either a strained or ordered structure, possibly similar to that encountered in crystals. An important aspect here is that the repeat unit is a large micelle ball, which is several tens of nanometers in diameter. Although both latex particles and block copolymer micelles in solution show a tendency to order into crystal-like structures in certain ranges of temperature and concentration (21), we are not aware of any micelle or latex systems that spontaneously forms macroscopic needles on drying.

REFERENCES AND NOTES

1. D. W. R. Gruen, *J. Phys. Chem.* **89**, 146 (1985); E. W. Kaler, A. K. Murthy, B. E. Rodriguez, J. A. N. Zasadzinski, *Science* **245**, 1371 (1989); S. A. Safran, P. Pincus, D. Andelman, *ibid.* **248**, 354 (1990); J. N. Israelachvili, *Intermolecular and Surface Forces* (Academic Press, London, ed. 2, 1992).
2. T. Inoue, T. Soen, T. Hashimoto, H. Kawai, in *Block Copolymers*, S. L. Aggarwal, Ed. (Plenum, New York, 1970), pp. 53-78; R. A. Brown, A. J. Masters, C. Price, X. F. Yuan, in *Comprehensive Polymer Science: Polymer Properties*, S. G. Allen, J. C. Bevington, C. Booth, C. Price, Eds. (Pergamon, Oxford, 1989), vol. 2, pp. 155-198.
3. E. L. Thomas *et al.*, *Macromolecules* **19**, 2197 (1986); H. Hasegawa, H. Tanaka, K. Yamasaki, T. Hashimoto, *ibid.* **20**, 1651 (1987); S. Forster *et al.*, *ibid.* **27**, 6922 (1994).
4. D. J. Kinning, K. I. Winey, E. L. Thomas, *ibid.* **21**, 3502 (1988).
5. J. Zhu, R. B. Lennox, A. Eisenberg, *J. Phys. Chem.* **96**, 4727 (1992).
6. C. Price, in *Developments in Block Copolymers*, I. Goodman, Ed. (Applied Science, London, 1982), vol. 1, pp. 39-80; J. Selb and Y. Gallot, *ibid.* (Applied Science, London, 1985), vol. 2, pp. 27-96.
7. Z. Tuzar and P. Kratochvil, in *Surface and Colloid Science*, E. Matijevic, Ed. (Plenum, New York, 1993), vol. 15, pp. 1-83.
8. C. Price, *Pure Appl. Chem.* **55**, 1563 (1983); A. P. Gast, P. K. Vinson, K. A. Cogan-Farinas, *Macromolecules* **26**, 1774 (1993); M. Antonietti, S. Heinz, M. Schmidt, C. Rosenauer, *ibid.* **27**, 3276 (1994).
9. R. Hilfiker, D. Q. Wu, B. Chu, *J. Colloid Interface Sci.* **135**, 573 (1990); C. Honda, K. Sakaki, T. Nose, *Polymer* **35**, 5309 (1994).
10. X. F. Zhong, S. K. Varshney, A. Eisenberg, *Macromolecules* **25**, 7160 (1992).
11. For the observations of the size and size distribution of the block copolymer aggregates, solution samples were deposited from solution onto copper EM grids that had been precoated with a thin film of Formvar (J.B.EM Services Inc.) and then coated with carbon. Water was evaporated from the grid for 1 day at atmospheric pressure, and the grids were shadowed with a palladium-platinum alloy at a shadowing angle of 33°. Core diameters were measured directly from prints of the microscope negatives and confirmed by measurement of the shadow length. For the observation of the internal morphology of the complex micelles, a powder sample of the complex

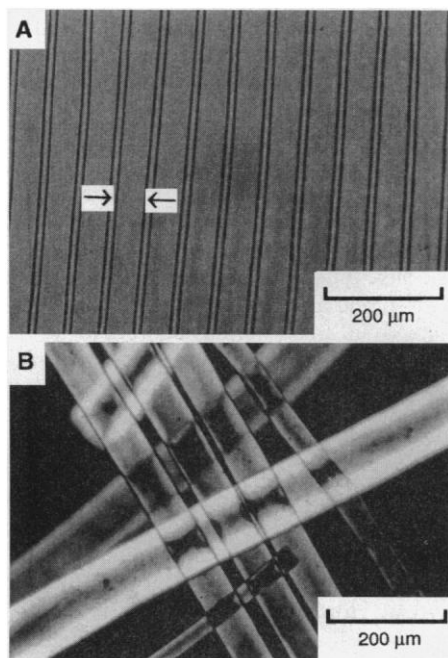


Fig. 4. The needle-like solid formed by drying an aqueous solution of the spherical micelles of the 180-*b*-28 diblock copolymer at 60°C. (A) An optical micrograph shows the crack pattern which forms the needles. The arrows indicate the dimension of a single needle. (B) An optical micrograph (taken using crossed polarized light) of the needles after soaking in water.

- micelles was embedded in epoxy resin (Epon), and thin sections of ~60 nm in thickness were obtained by microtoming the resin sample at room temperature. In order to increase the contrast between the PAA and the PS regions, the sections were stained with CsOH (aq) and washed with deionized water to remove excess CsOH.
12. A. Halperin, M. Tirrell, T. P. Lodge, *Adv. Polym. Sci.* **100**, 31 (1992).
 13. Z. Gao, S. K. Varshney, S. Wong, A. Eisenberg, *Macromolecules* **27**, 7923 (1994).
 14. A. Desjardins and A. Eisenberg, *ibid.* **24**, 5779 (1991).
 15. D. Nguyen, C. Williams, A. Eisenberg, *ibid.* **27**, 5086 (1994).
 16. A. E. Platt, in *Comprehensive Polymer Science: Polymer Reactions*, S. G. Allen, J. C. Bevington, G. C. Eastmond, A. Ledwith, S. Russo, P. Sigwalt, Eds. (Pergamon, Oxford, 1989), vol. 6, chap. 14.
 17. L. Zhang, R. J. Barlow, A. Eisenberg, unpublished results.

18. M. D. Whitmore and J. Noolandi, *Macromolecules* **18**, 657 (1985); R. Nagarajan, K. Ganesh, *J. Chem. Phys.* **90**, 5843 (1989).
19. A. Halperin, *Macromolecules* **20**, 2943 (1987); D. Ronis, *Phys. Rev. E* **49**, 5438 (1994).
20. M. R. Munch and A. P. Gast, *Macromolecules* **21**, 1360 (1988); A. M. Mayes and M. O. de la Cruz, *ibid.* **21**, 2543 (1988); A. Ajdari and L. Leibler, *ibid.* **24**, 6803 (1991); Z.-G. Wang, *ibid.* **25**, 3702 (1992).
21. M. Shibayama, T. Hashimoto, H. Kawai, *Macromolecules* **16**, 16 (1983); N. Ise, *Angew. Chem. Int. Ed. Engl.* **25**, 323 (1986); P. N. Pusey and W. van Meegen, *Nature* **320**, 340 (1986); G. A. McConnell, A. P. Gast, J. S. Huang, S. D. Smith, *Phys. Rev. Lett.* **71**, 2102 (1993).
22. We thank R. J. Barlow and M. Topors for useful discussions. We also thank The Natural Science and Engineering Research Council of Canada (NSERC) for continuing support of this research.

21 February 1995; accepted 27 April 1995

Calorimetric Measurement of the Energy Difference Between Two Solid Surface Phases

Y. Y. Yeo, C. E. Wartnaby, D. A. King

A recently designed single-crystal surface calorimeter has been deployed to measure the energy difference between two solid surface structures. The clean Pt{100} surface is reconstructed to a stable phase in which the surface layer of platinum atoms has a quasi-hexagonal structure. By comparison of the heats of adsorption of CO and of C₂H₄ on this stable Pt{100}-hex phase with those on a metastable Pt{100}-(1×1) surface, the energy difference between the two clean phases was measured as 20 ± 3 and 25 ± 3 kilojoules per mole of surface platinum atoms.

Phase transitions in bulk systems can be readily characterized by their enthalpy change by using calorimetric measurements. Although surface phase transitions are well known, their energetics have been inferred indirectly, either through kinetics measurements (1) or by theoretical studies (2), or both. Recently we have developed a surface calorimeter that allows heats of adsorption to be measured directly (3). Because chemisorption can induce or lift surface reconstructions, such studies can be used to construct thermodynamic cycles that allow the heat of the surface reconstruction to be determined directly. Because of recent developments in the theoretical treatment of metal surfaces, it is of great importance to obtain such high-quality experimental data, which can serve as a testing ground for theory.

The clean Pt{100} surface can be prepared in a metastable ideal bulk termination (1×1) structure, stable at 300 K. On heating above 500 K, the surface reconstructs to a more stable structure, in which the top layer adopts a quasi-hexagonal structure and the second layer retains the square array of the {100} surface. This phase

is referred to as Pt{100}-hex, following Heilmann *et al.* (4). Adsorption of several gases, including CO, NO, and H₂, induces a reversal of this surface to the (1×1) phase, a process that plays a critical role in the catalytic reactions on this surface, including the phenomena of bistability and kinetic oscillations (5). Recently, the growth rate of (1×1) islands on the hex phase was found to follow a strongly nonlinear power law dependence on the CO (6) and H (7) coverages on the hex phase. The energetics of the hex and (1×1) phases of Pt{100} have recently been computed with the use of density functional theory (8), making this an appropriate system for experimental study.

Our methodology for determining the surface phase transition energy is as follows. The clean metastable Pt{100}-(1×1) and the stable Pt{100}-hex surfaces are prepared by the standard procedures (9), and the calorimetric heats of adsorption of CO and of C₂H₄ are measured on each of these surfaces, in turn, as a function of surface coverage. The term "differential heat of adsorption" refers to the heat released in an incremental adsorption following a path in which no work is performed; as in our calorimetric experiments, it is identical to the isosteric heat defined by constant-coverage

pressure-temperature equilibrium (10). The integral heat of adsorption ΔH_{in} can then be calculated from the differential heat ΔH_{diff} by summing the coverage-differential heat product and then normalizing this result against the coverage θ

$$\Delta H_{in} = \frac{\int \Delta H_{diff} d\theta}{\int d\theta}$$

At 300 K, adsorption on the hex phase leads to rapid conversion to the (1×1) structure, such that the final state at θ_{co} = 0.5 monolayer (ML) is the same in each case. Evidence for this conclusion is provided by the loss of the hex pattern and the appearance of a c(4×2) low-energy electron diffraction (LEED) pattern (11). Confirmation is provided in an infrared study carried out by Martin *et al.* (12) in which identical bands were observed at 1869 cm⁻¹ (weak) and 2088 cm⁻¹ (sharp) after adsorption of 0.5 ML of CO onto both the hex and (1×1) surfaces. The differential heats of adsorption also coincided, within experimental error, at CO coverages exceeding 0.5 ML, further substantiating the conclusion that the same final state was attained. The difference between the two heats of adsorption is therefore the difference in surface energies between the (1×1) and the hex phases of the clean surface. The CO differential heats of adsorption -ΔH_{diff} are shown in Fig. 1. Because the heats are expressed per mole of CO molecules and because, for a total coverage θ_{co} = 0.5 ML, there are two surface Pt atoms (Pt_s) for each adsorbed CO molecule, the integral adsorption heats of CO are halved to represent the heat per mole of Pt_s atoms

$$\begin{aligned} \text{Pt}_s\{100\}\text{-hex} + \text{CO(g)} &\rightarrow \text{Pt}\{100\}\text{-(1}\times\text{1)} \\ &- \text{CO}(\theta_{\text{co}} = 0.5) - \Delta H_{in}^{\text{hex}} \\ &= 85 \pm 2 \text{ kJ (mol Pt}_s\text{)}^{-1} \end{aligned}$$

$$\begin{aligned} \text{Pt}_s\{100\}\text{-(1}\times\text{1)} + \text{CO(g)} &\rightarrow \text{Pt}\{100\}\text{-(1}\times\text{1)} \\ &- \text{CO}(\theta_{\text{co}} = 0.5) - \Delta H_{in}^{1\times 1} \\ &= 105 \pm 2 \text{ kJ (mol Pt}_s\text{)}^{-1} \end{aligned}$$

where -ΔH_{in}^{hex} is the integral heat of adsorption on the hex phase at θ_{CO} = 0.5 ML and -ΔH_{in}^{1×1} is the integral heat of adsorption on the (1×1) phase at θ_{CO} = 0.5 ML. Thus, the energy difference between the two clean surface phases is 20 ± 3 kJ (mol Pt_s)⁻¹. This can also be expressed as 0.43 J m⁻² or 0.21 eV per (1×1) area.

Any adsorbate that efficiently converts the hex phase of Pt{100} to the (1×1) phase should give the same result for the surface energy difference. In Fig. 2, we show calorimetric (that is, differential) adsorption heat measurements for C₂H₄ adsorption on Pt{100} hex and (1×1) phases. As for CO adsorption, there is a significant difference at low coverages, and the heats become

Department of Chemistry, University of Cambridge, Cambridge CB2 1EW, UK.